Materials Today Chemistry 1-2 (2016) 32–39

Contents lists available at ScienceDirect

Materials Today Chemistry

journal homepage: www.journals.elsevier.com/materials-today-chemistry/

Rough-surfaced molybdenum carbide nanobeads grown on graphene-coated carbon nanofibers membrane as free-standing hydrogen evolution reaction electrocatalyst

Wei Gao [a], Yiqin Shi [b], Lizeng Zuo [a], Wei Fan [b, **], Tianxi Liu [a, b, *]

[a] State Key Laboratory of Molecular Engineering of Polymers, Department of Macromolecular Science, Fudan University, 220 Handan Road, Shanghai 200433, PR China

[b] State Key Laboratory for Modification of Chemical Fibers and Polymer Materials, College of Materials Science and Engineering, Donghua University, 2999 North Renmin Road, Shanghai 201620, PR China

ARTICLE INFO

Article history:
Received 31 August 2016
Received in revised form
3 October 2016
Accepted 4 October 2016

Keywords:
Molybdenum carbide
Nanobeads
Graphene-coated carbon nanofibers membrane
Free-standing
Hydrogen evolution reaction

ABSTRACT

A novel free-standing pie-like paper electrode composed of Mo_2C nanobeads on graphene-coated carbon nanofibers (G-CNF) membrane was rationally designed as advanced electrocatalyst for hydrogen evolution reaction (HER). A thin layer of graphene is coated on the surface of CNF membrane, forming a "crust" on fibrous web architecture. The unique design of the all-carbon membrane, which is a 3D interconnected conductive framework of nanofibers, reduces the resistance of electron and ion transport during the electrocatalyzing process. With G-CNF performing as support, well-shaped Mo_2C nanobeads were immobilized on the fibers through hydrothermal and calcination procedures, offering rich catalytic sites on the exposed rough surface. Owing to all these merits, the composite membrane of Mo_2C-G-CNF exhibits high HER catalytic activity with onset potential of 115 mV in acidic solution and 108 mV in basic solution. Furthermore, the good durability in both acidic and basic environment guarantees its practical application as free-standing electrode material.

1. Introduction

As hydrogen is considered as indispensable greenhouse gas-free fuel in the future [1], a lot of attentions have been devoted by researchers to hydrogen evolution from electrolysis of water. Seeking for inexpensive and highly efficient hydrogen evolution reaction (HER) catalysts as alternatives for costly and scarce platinum based catalysts is urgent for sustainable and large scale hydrogen production [2]. Molybdenum carbide (Mo_2C) has recently been explored as one promising candidate owing to its Pt-resembling electronic structure achieved by the introduction of carbon into the lattice of molybdenum [3] and the earth abundant characteristic. However, commercial available Mo_2C is inadequate for satisfying the demand of practical applications. Various strategies have been employed to improve the reliability and activity of Mo_2C, such as nanostructuring [4,5], heteroatom doping to increase active sites [6,7] and exploiting hybrid structure [8,9]. Among them, controllable synthesis of Mo_2C with carefully selected support such as graphene porous foam [10], nitrogen-rich nanocarbon [11] and carbon cloth [12] is a direct and efficient approach that could gain reduced grain size and render uniform distribution of Mo_2C to realize the optimization of its catalytic activity.

As one of the typical carbon supports, one-dimensional carbon nanofibers (CNFs) are intensively studied as supports to construct free-standing electrodes for HER electrocatalysis [13–15]. Electrospinning stands out as an effective support method due to its easy accessibility for mass production of nanofibers with high surface to volume ratio [16–18]. The morphologies and properties of CNFs can be flexibly adjusted by controlling the processing condition. Benefiting from these advantages, the electrospun CNFs have found a wide range of applications in energy storage and conversion fields like lithium ion battery [19], sensing [20] and electrocatalyzing [21]. However, the isolation of fibers in the electrospun membrane imposes limit on its conductivity, thus influences its electrochemical performance. A library of methods has been employed to

* Corresponding author. State Key Laboratory of Molecular Engineering of Polymers, Department of Macromolecular Science, Fudan University, 220 Handan Road, Shanghai 200433, PR China.

** Corresponding author.

E-mail addresses: weifan@dhu.edu.cn (W. Fan), txliu@fudan.edu.cn, txliu@dhu.edu.cn (T. Liu).

http://dx.doi.org/10.1016/j.mtchem.2016.10.003
2468-5194/

improve the conductivity of carbon nanofibers like incorporation of carbon nanomaterials [22] and metallic nanoparticles [23]. However, these methods require complex procedures and can hardly realize uniform dispersion of additives in the fibers. Adding conductive coating, has been developed as a more convenient and effective strategy that could overcome these shortcomings [24]. Two-dimensional graphene, with theoretically superior conductivity, large surface area, outstanding mechanical properties and excellent chemical stability, is an ideal coating agent for enhancing conductivity of the electrode material [25,26].

Herein, we have constructed the composite membrane of graphene-coated carbon nanofibers (G-CNF) membrane using electrospinning and dip-coating method with subsequent carbonization [27,28]. The as-obtained G-CNF membrane with rationally designed architecture then acts as conductive support for *in-situ* growth of Mo_2C through a typical hydrothermal method and high temperature carbonization procedure. Mo_2C nanobeads with rough surface, as key catalytic components, are uniformly anchored on the fibrous framework and afford abundant active sites where HER could proceed. Graphene layers interconnect with each other and tightly adhere to CNFs, forming a conductive plane to reduce the resistance of electron/ion transport in the catalyst. CNFs, acting as spacer, prevent the severe stacking of graphene to give full play of its conductivity. The three-dimensional fibrous web and crimpled surface of G-CNF could provide a lot of sites for anchoring Mo_2C. The resultant composite membrane of Mo_2C-G-CNF exhibits prominent catalytic activity with good stability in both acidic and basic media, being a promising candidate for high-performance HER catalysis.

2. Materials and methods

2.1. Materials

Polyacrylonitrile (PAN) (Mw = 150 000 g mol^{-1}) was purchased from Sigma-Aldrich. H_2SO_4 (95–98%), H_2O_2 (30%), HNO_3 (65%), ethanol, *N*,*N*-dimethylformamide (DMF, ≥99.5%), sodium hydrate (NaOH), glucose, potassium permanganate ($KMnO_4$) and ammonium molybdate ($(NH_4)_6Mo_7O_{24}\cdot 4H_2O$) were purchased from Sinopharm Chemical Reagent Co., Ltd. Natural graphite powder (325 mesh) was obtained from Alfa-Aesar (Ward Hill, MA) and used without further purification. Deionized (DI) water was used throughout all the experiments.

2.2. Preparation of graphene-coated carbon nanofibers membrane (G-CNF)

PAN nanofiber membrane was first fabricated by a simple single-nozzle electrospinning technique. Typically, 1 g of PAN was dissolved in 5 mL of DMF by heating at 70 °C for 3 h under vigorous stirring to form viscous transparent solution and subsequently transferred to a 5 mL syringe. The electrospinning was conducted at an applied voltage of 20 kV with a feeding rate of 0.25 mm min^{-1} through a stainless steel needle positioned 20 cm away from the aluminum drum collector. The as-obtained PAN nanofiber membrane was preoxidized at 250 °C in air atmosphere for 2 h with a ramping rate of 2 °C min^{-1}. Then, the preoxidized PAN (o-PAN) membrane was cut into small pieces with size of 2 cm × 2 cm and dipped in graphene oxide (GO) solution (2 mg mL^{-1}) for 2 h to allow GO sheets to assemble on the membrane to form a layered coating. After being washed with ethanol and dried, the GO coated o-PAN membrane was placed in a tube furnace for carbonization at 800 °C for 2 h under N_2 atmosphere to obtain G-CNF membrane.

2.3. Preparation of Mo_2C nanobeads loaded G-CNF (Mo_2C-G-CNF) membrane

The as-obtained G-CNF membrane was first acidized by being immersed into HNO_3 solution (30%) and heated at 40 °C for 12 h. Then the membrane was rinsed with water for several times and dried under 70 °C. A certain amount of $(NH_4)_6Mo_7O_{24}\cdot 4H_2O$ and glucose with weight ratio of 4:1 was dissolved in 40 mL H_2O. The acid-treated G-CNF membrane was immersed into the above solution and subsequently transferred into 100 mL Teflon stainless-steel autoclave, reacting at 180 °C for 12 h. The membrane was collected by tweezers, repeatedly washed with DI water and ethanol, and finally dried under 60 °C overnight. Afterwards, the samples were carbonized at 900 °C under N_2 atmosphere for 2 h with a heating rate of 5 °C min^{-1} to get the final product of Mo_2C-G-CNF membrane. For comparison, pure Mo_2C was synthesized by the same synthetic method except that no support was introduced. Mo_2C directly grown on carbon nanofiber membrane (Mo_2C-CNF) was also fabricated where the step of dip coating GO was eliminated.

2.4. Characterization

The morphology of samples was characterized by field emission scanning electron microscopy (FESEM) (Ultra 55, Zeiss) at an acceleration voltage of 5 kV. The chemical composition was characterized by the energy dispersive X-ray spectroscopy (EDX). Raman spectra were measured on a JobinYvon XploRA Raman spectrometer at an exciting wavelength of 632.8 nm. X-ray diffraction (XRD) patterns were obtained on an X'Pert Pro X-ray diffractometer with Cu Kα radiation (λ = 0.1542 nm) under a current of 40 mA and a voltage of 40 kV with 2θ ranges from 5° to 80°. X-ray photoelectron spectroscopy (XPS) analyses were performed on a VG ESCALAB 220I-XL device and all XPS spectra were corrected using C1s line at 284.5 eV. In addition, the curve fitting and background subtraction were accomplished using XPS PEAK41 software. Thermogravimetric analysis (Pyris 1 TGA) was performed under air flow from 100 to 800 °C at a heating rate of 20 °C min^{-1}.

2.5. Electrochemical measurements

Before all the hydrogen evolution experiments, glassy carbon electrodes (GCE) (diameter: 5 mm) were pretreated according to the previous report [29]. The working electrode was prepared as follows: The Mo_2C-G-CNF membrane was cut into small pieces with size of 5 mm × 5 mm and adhered to GCE by using 5 μL of 5 wt% nafion, then dried at room temperature to achieve Mo_2C-G-CNF membrane modified GCE. To prepare Mo_2C modified GCE, 2 mg of pure Mo_2C powder was dispersed in 1 mL DMF/DI water mixed solution (volume ratio: 3:1) containing 20 μL 5 wt% nafion. Then, the mixture was sonicated for 2 h to get the homogeneous slurry. Finally, 10 μL of the slurry was dropped onto GCE and dried. All electrochemical tests were conducted on a CHI 660D electrochemical workstation (Chenhua Instruments Co, Shanghai, China) with standard three-electrode setup at room temperature, where sample modified GCE was applied as the working electrode, saturated calomel electrode (SCE) as the reference electrode and Pt wire as counter electrode. The hydrogen evolution performance tests were performed by liner sweep voltammetry (LSV) in nitrogen purged electrolyte solution of 0.5 M H_2SO_4 and 1 M NaOH, respectively, with scan rate of 2 mV s^{-1}. The double-layer capacitance (C_{dl}) of electrocatalyst was measured by scanning the cyclic voltammograms in the range of 0.1–0.3 V vs. RHE. By plotting the j_a-j_c at 0.2 V vs. RHE against the scan rate, C_{dl} was estimated as half of the slope. Electrochemical impedance spectroscopy (EIS) measurements were

conducted in 0.5 M H_2SO_4 from 0.01 Hz to 100 Hz at the potential of 200 mV with the amplitude of 5 mV. The durability tests were performed by measuring the time dependent current density curves under a certain applied overpotential in both 0.5 M H_2SO_4 and 1 M NaOH. All the potentials were calibrated to RHE according to the equation of $E_{RHE} = E_{SCE} + (0.241 + 0.059\ pH)$ V.

3. Results and discussion

3.1. Morphology and structure of Mo_2C-G-CNF

CNFs, which were achieved by carbonization of o-PAN nanofibers, have smooth surface and long flexuous morphology with a diameter of approximate 200 nm, interconnecting with each other to construct a three-dimensional web (Fig. 1A and C). As o-PAN nanofibers were dipped into GO solution, GO sheets were assembled on the surface of nanofibers through the interactions between amino groups of o-PAN nanofibers and the carboxyl groups on the plane of GO, forming a layered coating on the fibrous web. After carbonization, GO layers were thermally reduced to graphene retaining the overall coverage on the o-PAN derived CNF membrane. From SEM images of G-CNF (Fig. 1B and D), a continuous wavy film can be observed, consisting of interconnected few-layered graphene sheets that closely adhere to the surface of the CNF membrane. In this way, the isolated CNFs are interconnected together by GO sheets, displaying a much rougher surface as well as slight deformation probably caused by the squeezing effect of graphene layers. Besides, no breakage is observed, indicating that the membrane maintains its integrity during the dip coating process. This unique architecture of crust on fibrous web could enhance the conductivity of the whole membrane (the electrical conductivity is 0.078 S cm^{-1} for bare CNF membrane and 0.191 S cm^{-1} for G-CNF membrane), thus facilitating the electron/ion transport during the electrochemical reaction. Furthermore, adhering to fibers in reverse prevents graphene from severe restacking and brings wrinkles on graphene layers, resulting in a continuous wavy plane, which could offer more anchoring sites.

The successful coating of graphene on CNF membrane can also be revealed by the Raman spectra (Fig. 2). All the three samples of bare CNF membrane, graphene powders and G-CNF membrane display two characteristic bands: D band at 1350 cm^{-1} and G band at 1590 cm^{-1}, indicating the disordered carbon and sp^2-bonded carbon atoms, respectively. For bare CNF membrane, the intensity ratio of G band (I_G) to D band (I_D) is 0.92, while that of pure graphene powder is 1.07. I_G/I_D is evaluated to be 0.95 for the G-CNF composite membrane, which is the intermediate value of its two individual components, indicating they couple well with each other.

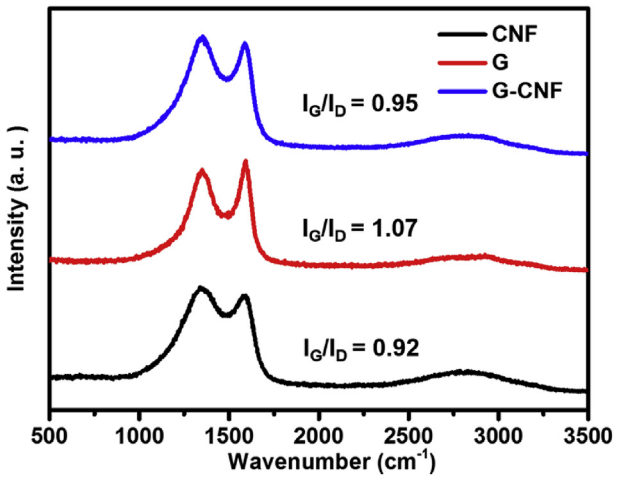

Fig. 2. Raman spectra of pure CNF membrane, graphene and G-CNF membrane.

The G-CNF membrane was then acidized to improve hydrophilicity for *in-situ* growing of Mo_2C through a typical hydrothermal method and subsequent high temperature carbonization. Without any supports, pure Mo_2C synthesized through the same procedure will grow into clusters, which hinder the exposure of active surface to the electrolyte (Fig. 3A and B). When acid-treated CNF membrane is introduced as supporting material, Mo_2C tends to grow into regular-shaped nanobeads strung on the nanofibers with rough surface (Fig. 3C and D, Fig. S1). In the case of Mo_2C-G-CNF composite membrane, roughly surfaced Mo_2C nanobeads with

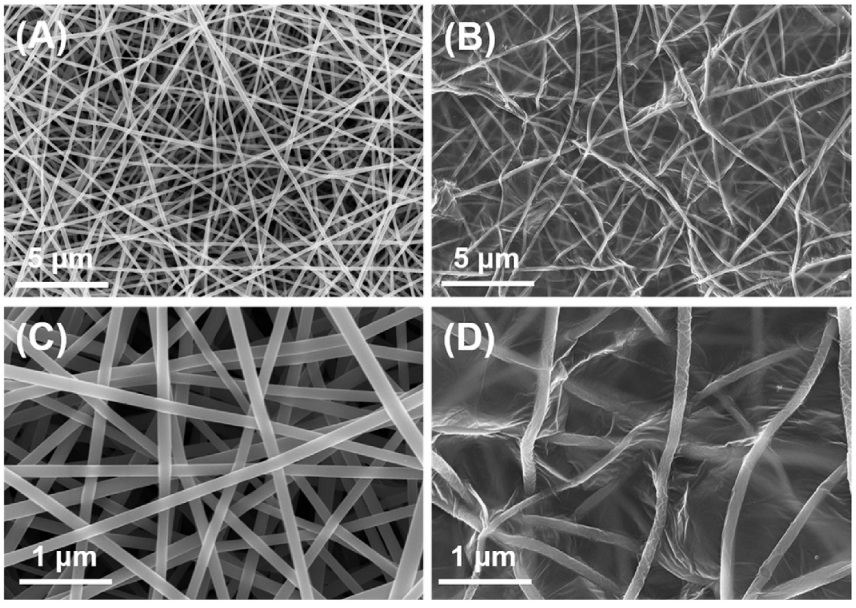

Fig. 1. SEM images of (A, C) pure CNF membrane and (B, D) G-CNF membrane at low and high magnifications.

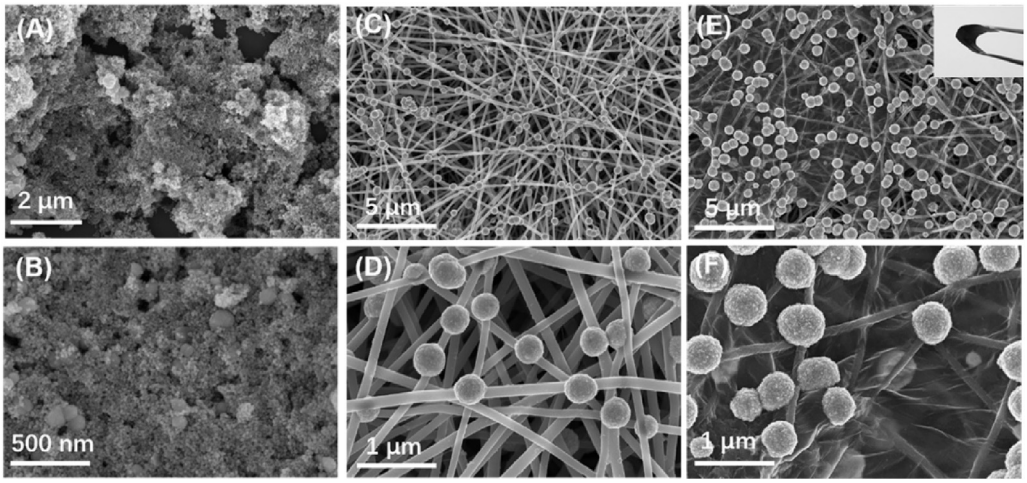

Fig. 3. SEM images of (A, B) pure Mo_2C, (C, D) Mo_2C-CNF and (E, F) Mo_2C-G-CNF at low and high magnifications.

diameter of approximate 400 nm are anchored on the G-CNF with pie-like structure (Fig. 3E and F). Besides, the composite membrane exhibits good mechanical flexibility as shown in the inset in Fig. 3E. Since the crumbled graphene layer could afford more anchoring sites as a substrate, Mo_2C nanobeads grow more densely on both of the top and bottom faces of G-CNF than on those of pure CNF membrane, which are predicted to offer more catalytic sites. Furthermore, few small gaps can be observed on the graphene plane, which could render solution permeation into the inner membrane structure, avoiding complete sealing of G-CNF membrane. In this way, the precursor solution can still impregnate the inner structure and guarantee the growth of Mo_2C nanobeads on the inner fibers. Cross sectional SEM images evidence the successful immobilization of Mo_2C nanobeads on these inner fibers beneath the graphene surface, and the whole membrane displays a hierarchical architecture (Fig. 4A). Notably, those Mo_2C beads incline to locate in the junctions of two or more fibers (Fig. 4B), which could contribute to improve the electron transfer rate of composite membrane considering the intrinsic high electrical conductivity of Mo_2C [30,31]. EDX results demonstrate the uniform Mo distribution in Mo_2C nanobeads, while element of C can be detected from both carbide nanobeads and the support of G-CNF membrane. The low content of O can be probably attributed to slight oxidation of Mo_2C surface as being exposed to air (Fig. 5). The loading of Mo_2C on the G-CNF membrane is estimated to be 9.91% through TGA analysis (Fig. S2).

XRD patterns of pure Mo_2C, as well as the membranes of CNF, G-CNF and Mo_2C-G-CNF are presented in Fig. 6. Except for the broad peak assigned to (002) plane of carbon that could also be observed in CNF and G-CNF, the composite membrane of Mo_2C-G-CNF displays the same sharp peaks as that of pure Mo_2C. These peaks positioned at $2\theta = 34.8°$, $38.2°$, $39.8°$, $52.5°$, $62.0°$, $70.0°$, $75.1°$ and $76.0°$ are indexed to (100), (002), (101), (102), (110), (103), (112) and (201) facets of hexagonal β-Mo_2C (JCPSD No. 00-035-0787), the most active phase for HER electrocatalysis among the four phases of molybdenum carbide [32].

The composition and surface valence state of Mo_2C-G-CNF are elucidated by XPS analysis. The survey spectrum indicates the presence of C, O, and Mo as main elements in the composite membrane (Fig. 7A). The deconvoluted spectrum of C 1s is shown in Fig. 7B, revealing peaks at 284.7, 285.4, 286.4 eV which belong to C—C, C═C bonds and oxygen-containing C—O bonds, respectively. Molybdenum bonded carbon in Mo_2C is manifested by the peak at lower binding energy of 284.1 eV. The high-resolution spectrum of Mo 3d reveals peaks at 228.9 and 233.0 eV stemmed from Mo_2C (Fig. 7C) [33]. In parallel, due to the surface oxidation as being exposed to air or during high energy XPS tests, peaks at 232.4 eV and 236 eV can be attributed to the oxides, MoO_x. In the deconvoluted O 1s spectrum, these two split peaks at 530.2 eV and 531.0 eV can be attributed to Mo—O bonds and peaks at 532.0 and 533.0 eV represent C═O bond and C—O bond, respectively (Fig. 7D).

3.2. HER electrocatalytic activity of Mo_2C-G-CNF composite membrane

The electrocatalytic activity of Mo_2C-G-CNF towards HER in acidic environment is evaluated by adopting a three-electrode system in 0.5 M H_2SO_4 at 2 mV s^{-1}. The performance of pure Mo_2C, the all-carbon membrane of G-CNF and Mo_2C-CNF membrane without graphene coating is also assessed. Observed from the

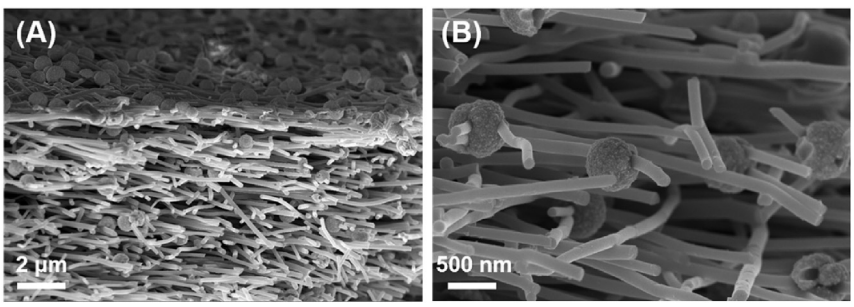

Fig. 4. Cross-sectional SEM images of Mo_2C-G-CNF membrane at (A) low and (B) high magnifications.

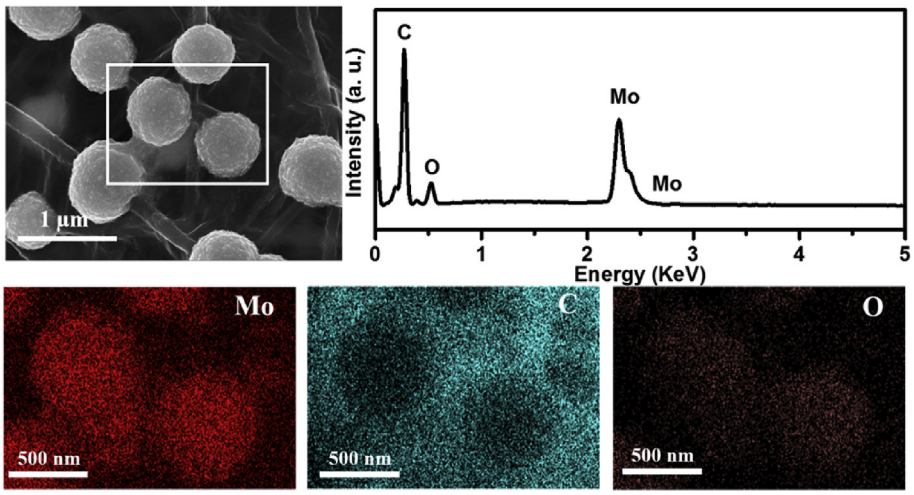

Fig. 5. EDX results of Mo_2C-G-CNF membrane: EDX spectrum taken from the selected area and the elemental mapping for Mo, C and O.

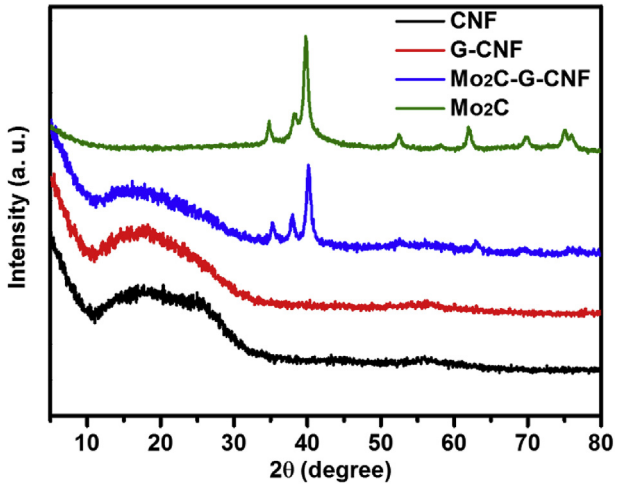

Fig. 6. XRD patterns of pure Mo_2C, CNF, G-CNF and Mo_2C-G-CNF membranes.

LSV curves, the all-carbon G-CNF membrane exhibits almost no HER catalytic effect as its LSV curve approaches a horizontal line. Although all of Mo_2C, Mo_2C-CNF and Mo_2C-G-CNF show distinct HER catalytic performance, Mo_2C exhibits inferior performance than the other two due to the lack of conductive supports for anchoring and avoiding the aggregation. For Mo_2C-G-CNF, these well-shaped Mo_2C nanobeads could join fibers together, enhancing the conductivity. Furthermore, the rough surface of nanobeads could increase the exposed active sites to catalyze HER. It is notable that Mo_2C-G-CNF displays a smaller onset potential and lower cathodic current under the same applied potential than Mo_2C-CNF, verifying that the introduction of graphene on fibrous web could help to improve the catalytic activity (Fig. 8A). Graphene layer coated on the membrane could provide a conductive plane for enhancing electron/ion transfer. Additionally, the well-designed pie-like structure tends to anchor more Mo_2C nanobeads. Although graphene formed a layered coating on the surface of CNFs membrane, it does not completely seal the inner fibrous web. The small gaps on the surface could still allow the electrolyte to full impregnate the electrode material so that the electrocatalysis of HER could still proceed in the inner structure. The potential value for a current density of 10 mA cm^{-2} is generally accepted as an important reference because solar-light-coupled HER apparatuses usually operate at 10–20 mA cm^{-2} under standard conditions [33]. To drive such a current density, a smaller overpotential of 188 mV is required for Mo_2C-G-CNF membrane, compared with 274 mV for pure Mo_2C and 215 mV for Mo_2C-CNF membrane.

To make a better comparison of the HER performance of Mo_2C-G-CNF and Mo_2C-CNF, their double layer capacitances (C_{dl}), which are proportional to their electrochemical surface areas have been measured via cyclic voltammetry (Fig. S2). Mo_2C-G-CNF indeed presents a larger C_{dl} of 66.5 mF cm^{-2}, compared with that of Mo_2C-CNF, indicating the coating of graphene layer on the fibrous web could endow the composite with larger electroactive surface area.

To further elucidate the HER mechanism, Tafel plots of different samples are subtracted from LSV curves and fitted to the Tafel equation ($\eta = b \log(j) + a$, where b is the Tafel slope, and j is the current density) (Fig. 8B). The Tafel slopes evaluated for Pt, pure Mo_2C and Mo_2C-G-CNF are 31 mV $decade^{-1}$, 103 mV $decade^{-1}$ and 72 mV $decade^{-1}$, respectively. Notably, Mo_2C-G-CNF exhibits a smaller Tafel slope than pure Mo_2C, demonstrating the higher hydrogen generation efficiency, which can be ascribed to the confined growth of Mo_2C nanobeads that uniformly distributed onto the support and thereby edge-rich morphologies are formed for Mo_2C-G-CNF. The Tafel slope suggests HER on the Mo_2C-G-CNF composite membrane modified electrode probably proceeds via a Volmer-Heyovsky mechanism, where the discharge step (the Volmer reaction) is followed by a rate-limiting electrochemical desorption step (the Heyrovsky reaction) [34].

Electrochemical impedance spectroscopy (EIS) is carried out for both Mo_2C-CNF and Mo_2C-G-CNF membranes for comparison and the Nyquist plots are shown in Fig. 8C. It is obvious that Mo_2C-G-CNF displays smaller charge transfer resistance (R_{ct}) and solution resistance (R_s), as well as lower ion diffusion resistance manifested by its larger line slope than those of Mo_2C-CNF membrane without a layer of graphene coating. The lower impedance can be attributed to the improved conductivity of G-CNF by the incorporation of a conductive bridge comprised of thin graphene layers overlapping with each other on the fibrous web. The durability of Mo_2C-G-CNF membrane is evaluated by operating the electrode under a certain applied overpotential to obtain the time-dependent current density (Fig. 8D). The slight current fluctuation observed from the current density-time curve demonstrates the good stability of Mo_2C-G-CNF membrane during the HER process in acidic media. After the long-term test, the Mo_2C could still remain the spherical structure but

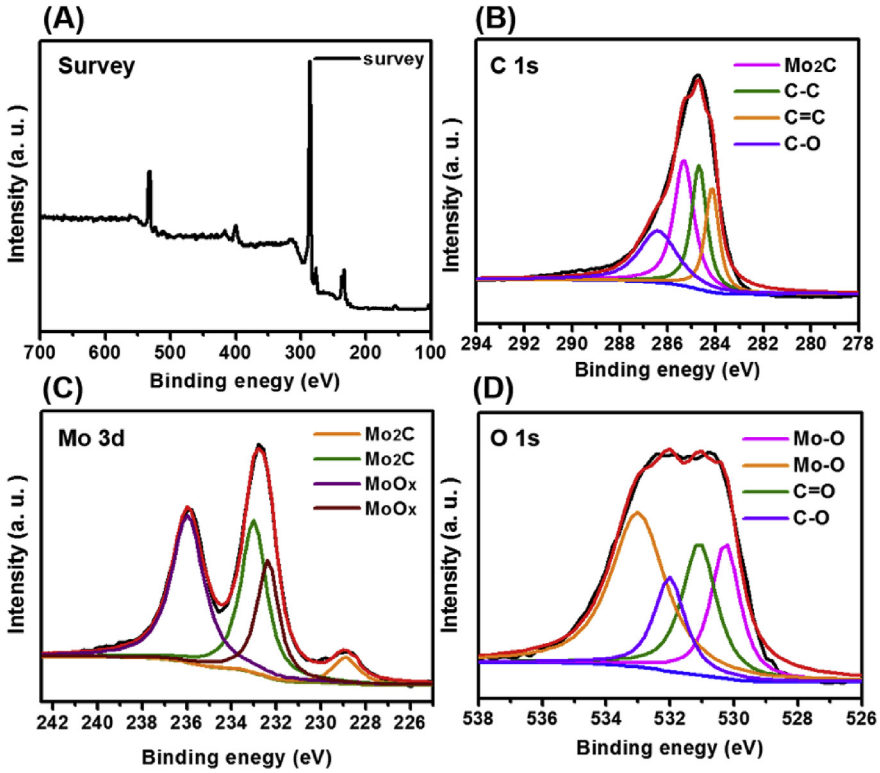

Fig. 7. XPS spectra of Mo_2C-G-CNF membrane: (A) survey spectrum; high-resolution (B) C 1s, (C) Mo 3d, and (D) O 1s spectra.

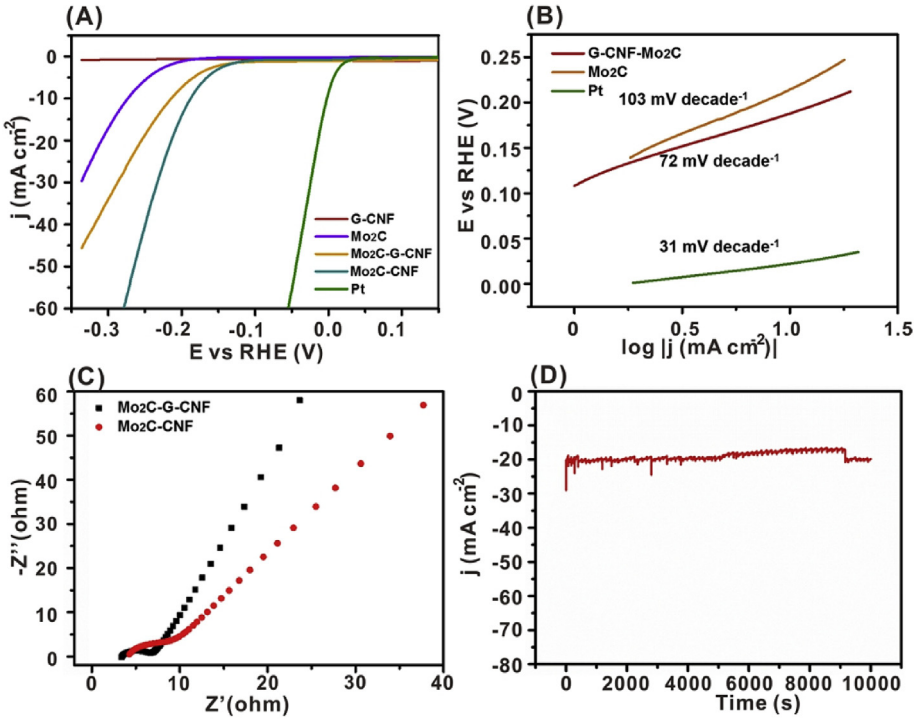

Fig. 8. (A) LSV polarization curves of pure Mo_2C, G-CNF, Mo_2C-CNF, Mo_2C-G-CNF membranes and Pt in N_2-purged 0.5 M H_2SO_4 solution. Scan rate: 2 mV s^{-1}. (B) Tafel plots of Mo_2C, Mo_2C-G-CNF and Pt. (C) Nyquist plots of Mo_2C-CNF and Mo_2C-G-CNF. (D) Time-dependent current density curve under $\eta = 370$ mV in 0.5 M H_2SO_4.

the surface has slight change (Fig. S4), which is probably due to the etching of oxides on the surface by the electrolyte.

Furthermore, the catalytic performance of Mo_2C-G-CNF in basic media is also evaluated by using the electrolyte of 1 M NaOH. As shown in the LSV curves in Fig. 9A, the current density

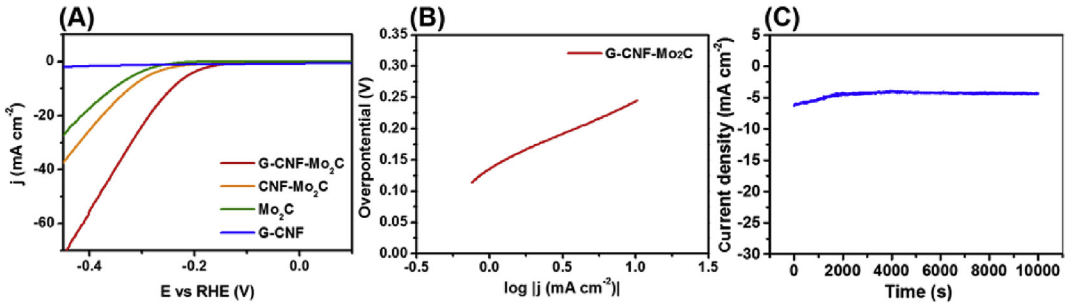

Fig. 9. (A) LSV polarization curves of pure Mo_2C, G-CNF, Mo_2C-CNF and Mo_2C-G-CNF membranes in N_2-purged 1 M NaOH solution. Scan rate: 2 mV s^{-1}. (B) Tafel plot of Mo_2C-G-CNF. (C) Time-dependent current density curve under $\eta = 420$ mV in 1 M NaOH.

corresponding to electrochemical hydrogen evolution increases more rapidly starting from smaller overpotential for Mo_2C-G-CNF membrane than other electrodes. And for driving a current density of 10 mA cm^{-2}, the overpotentials required for bare Mo_2C, Mo_2C-CNF and Mo_2C-G-CNF are 356, 322 and 241 mV, respectively, verifying that the composite membrane displays the highest catalytic activity in alkaline conditions. From the low current density region of the Tafel plot, the onset potential of Mo_2C-G-CNF is calculated to be 114 mV and the Tafel slope is estimated to be 108 mV $decade^{-1}$ (Fig. 9B). In addition, although the stability is not as good as that in acidic media indicated by the slight drop of current density in the initial stage (Fig. 9C), which is probably caused by the corrosion of carbide by NaOH, Mo_2C-G-CNF can still retain most of its performance during the long-term HER performance in the basic environment. The performance of our Mo_2C-G-CNF is better or comparable with previous reports (Table S1). Furthermore, the free-standing feature enables it to be more conveniently used as electrode material.

4. Conclusions

In summary, G-CNF membrane has been fabricated by dip-coating of o-PAN membrane with GO and subsequent carbonization. Then G-CNF is used as support for growing Mo_2C nanobeads. Those isolated nanobeads strung on the fibers with rough surfaces can offer abundant active catalytic sites, by coupling with graphene bound fibrous web that affords a fast pathway for electron/ion transfer, and the final product of Mo_2C-G-CNF bears optimized HER performance with good durability in both of the acidic and basic media. The all-carbon membrane of G-CNF with rationally designed pie-like architecture is elucidated as a promising support for fabricating highly conductive electrode materials for catalytic or capacitive applications.

Notes

The authors declare no competing financial interest.

Acknowledgements

The authors are grateful for the financial support from the National Natural Science Foundation of China (51125011, 51373037, 51433001).

Appendix A. Supplementary data

Supplementary data related to this article can be found at http://dx.doi.org/10.1016/j.mtchem.2016.10.003.

References

[1] L. Schlapbach, A. Züttel, Hydrogen-storage materials for mobile applications, Nature 414 (2001) 353–358.
[2] J.A. Turner, Sustainable hydrogen production, Science 305 (2004) 972–974.
[3] W.F. Chen, J.T. Muckerman, E. Fujita, Recent developments in transition metal carbides and nitrides as hydrogen evolution electrocatalysts, Chem. Commun. 49 (2013) 8896–8909.
[4] F.X. Ma, H.B. Wu, B.Y. Xia, C.Y. Xu, X.W. Lou, Hierarchical beta-Mo_2C nanotubes organized by ultrathin nanosheets as a highly efficient electrocatalyst for hydrogen production, Angew. Chem. Int. Ed. 54 (2015) 15395–15399.
[5] C. Tang, A. Sun, Y. Xu, Z. Wu, D. Wang, High specific surface area Mo_2C nanoparticles as an efficient electrocatalyst for hydrogen evolution, J. Power Sources 296 (2015) 18–22.
[6] H. Ang, H.T. Tan, Z.M. Luo, Y. Zhang, Y.Y. Guo, G. Guo, H. Zhang, Q. Yan, Hydrophilic nitrogen and sulfur co-doped molybdenum carbide nanosheets for electrochemical hydrogen evolution, Small 11 (2015) 6278–6284.
[7] C. Tang, W. Wang, A. Sun, C. Qi, D. Zhang, Z. Wu, D. Wang, Sulfur-decorated molybdenum carbide catalysts for enhanced hydrogen evolution, ACS Catal. 5 (2015) 6956–6963.
[8] B. Ma, H. Xu, K. Lin, J. Li, H. Zhan, W. Liu, C. Li, Mo_2C as non-noble metal co-catalyst in Mo_2C/CdS composite for enhanced photocatalytic H_2 evolution under visible light irradiation, ChemSusChem 9 (2016) 820–824.
[9] H. Lin, Z. Shi, S. He, X. Yu, S. Wang, Q. Gao, Y. Tang, Heteronanowires of MoC-Mo_2C as efficient electrocatalysts for hydrogen evolution reaction, Chem. Sci. 7 (2016) 3399–3405.
[10] J. Wang, H. Xia, Z. Peng, C. Lv, L. Jin, Y. Zhao, Z. Huang, C. Zhang, Graphene porous foam loaded with molybdenum carbide nanoparticle electrocatalyst for effective hydrogen generation, ChemSusChem 9 (2016) 855–862.
[11] Y. Liu, G. Yu, G.D. Li, Y. Sun, T. Asefa, W. Chen, X. Zou, Coupling Mo_2C with nitrogen-rich nanocarbon leads to efficient hydrogen-evolution electrocatalytic sites, Angew. Chem. Int. Ed. 54 (2015) 10752–10757.
[12] M. Fan, H. Chen, Y. Wu, L.L. Feng, Y. Liu, G.D. Li, X. Zou, Growth of molybdenum carbide micro-islands on carbon cloth toward binder-free cathodes for efficient hydrogen evolution reaction, J. Mater. Chem. A 3 (2015) 16320–16326.
[13] X. Zhang, L. Li, Y. Guo, D. Liu, T. You, Amorphous flower-like molybdenum-sulfide-@-nitrogen-doped-carbon-nanofiber film for use in the hydrogen-evolution reaction, J. Colloid Interface Sci. 472 (2016) 69–75.
[14] S. Yu, J. Kim, K.R. Yoon, J.W. Jung, J. Oh, I.D. Kim, Rational design of efficient electrocatalysts for hydrogen evolution reaction: single layers of WS_2 nanoplates anchored to hollow nitrogen-doped carbon nanofibers, ACS Appl. Mater. Interfaces 7 (2015) 28116–28121.
[15] Y. Shen, A.C. Lua, J.Y. Xi, X.P. Qiu, Ternary platinum-copper-nickel nanoparticles anchored to hierarchical carbon supports as free-standing hydrogen evolution electrodes, ACS Appl. Mater. Interfaces 8 (2016) 3464–3472.
[16] X. Mao, F. Simeon, G.C. Rutledge, T.A. Hatton, Electrospun carbon nanofiber webs with controlled density of states for sensor applications, Adv. Mater. 25 (2013) 1309–1314.
[17] B. Zhang, Y. Yu, Z. Huang, Y.B. He, D. Jang, W.S. Yoon, Y.W. Mai, F. Kang, J.K. Kim, Exceptional electrochemical performance of freestanding electrospun carbon nanofiber anodes containing ultrafine SnO_x particles, Energy Environ. Sci. 5 (2012) 9895–9902.
[18] H.R. Nie, C. Wang, A.H. He, Fabrication and chemical crosslinking of electrospun trans-polyisoprene nanofiber nonwoven, Chin. J. Polym. Sci. 34 (2016) 697–708.
[19] L. Qie, W.M. Chen, Z.H. Wang, Q.G. Shao, X. Li, L.X. Yuan, X.L. Hu, W.X. Zhang, Y.H. Huang, Nitrogen-doped porous carbon nanofiber webs as anodes for lithium ion batteries with a superhigh capacity and rate capability, Adv. Mater. 24 (2012) 2047–2050.
[20] X. Mao, X. Yang, G.C. Rutledge, T.A. Hatton, Ultra-wide-range electrochemical sensing using continuous electrospun carbon nanofibers with high densities of states, ACS Appl. Mater. Interfaces 6 (2014) 3394–3405.
[21] B. Jeong, D. Shin, M. Choun, S. Maurya, J. Baik, B.S. Mun, S.H. Moon, D. Su, J. Lee, Nitrogen-deficient ORR active sites formation by iron-assisted water vapor

activation of electrospun carbon nanofibers, J. Phys. Chem. C 120 (2016) 7705–7714.
[22] Y. Chen, X. Li, K. Park, J. Song, J. Hong, L. Zhou, Y.W. Mai, H. Huang, J.B. Goodenough, Hollow carbon-nanotube/carbon-nanofiber hybrid anodes for Li-ion batteries, J. Am. Chem. Soc. 135 (2013) 16280–16283.
[23] M. Zhi, A. Manivannan, F. Meng, N. Wu, Highly conductive electrospun carbon nanofiber/MnO_2 coaxial nano-cables for high energy and power density supercapacitors, J. Power Sources 208 (2012) 345–353.
[24] G. Yu, L. Hu, N. Liu, H. Wang, M. Vosgueritchian, Y. Yang, Y. Cui, Z. Bao, Enhancing the supercapacitor performance of graphene/MnO_2 nanostructured electrodes by conductive wrapping, Nano Lett. 11 (2011) 4438–4442.
[25] Z. Li, J.T. Zhang, Y.M. Chen, J. Li, X.W. Lou, Pie-like electrode design for high-energy density lithium-sulfur batteries, Nat. Commun. 6 (2015).
[26] G. Wang, Q. Dong, T. Wu, F. Zhan, M. Zhou, J. Qiu, Ultrasound-assisted preparation of electrospun carbon fiber/graphene electrodes for capacitive deionization: importance and unique role of electrical conductivity, Carbon 103 (2016) 311–317.
[27] D.D. Nguyen, N.H. Tai, S.B. Lee, W.S. Kuo, Superhydrophobic and superoleophilic properties of graphene-based sponges fabricated using a facile dip coating method, Energy Environ. Sci. 5 (2012) 7908–7912.
[28] J. Ge, H.B. Yao, W. Hu, X.F. Yu, Y.X. Yan, L.B. Mao, H.H. Li, S.S. Li, S.H. Yu, Facile dip coating processed graphene/MnO_2 nanostructured sponges as high performance supercapacitor electrodes, Nano Energy 2 (2013) 505–513.
[29] Y.P. Huang, H.Y. Lu, H.H. Gu, J. Fu, S.Y. Mo, C. Wei, Y.E. Miao, T.X. Liu, A CNT@$MoSe_2$ hybrid catalyst for efficient and stable hydrogen evolution, Nanoscale 7 (2015) 18595–18602.
[30] M. Ihsan, H. Wang, S.R. Majid, J. Yang, S.J. Kennedy, Z. Guo, H.K. Liu, MoO_2/Mo_2C/C spheres as anode materials for lithium ion batteries, Carbon 96 (2016) 1200–1207.
[31] C. Xu, L. Wang, Z. Liu, L. Chen, J. Guo, N. Kang, X.L. Ma, H.M. Cheng, W. Ren, Large-area high-quality 2D ultrathin Mo_2C superconducting crystals, Nat. Mater. 14 (2015) 1135–1141.
[32] K. Xiong, L. Li, L. Zhang, W. Ding, L. Peng, Y. Wang, S. Chen, S. Tan, Z. Wei, Ni-doped Mo_2C nanowires supported on Ni foam as a binder-free electrode for enhancing the hydrogen evolution performance, J. Mater. Chem. A 3 (2015) 1863–1867.
[33] J.S. Li, Y. Wang, C.H. Liu, S.L. Li, Y.G. Wang, L.Z. Dong, Z.H. Dai, Y.F. Li, Y.Q. Lan, Coupled molybdenum carbide and reduced graphene oxide electrocatalysts for efficient hydrogen evolution, Nat. Commun. 7 (2016).
[34] L. Liao, S. Wang, J. Xiao, X. Bian, Y. Zhang, M.D. Scanlon, X. Hu, Y. Tang, B. Liu, H.H. Girault, A nanoporous molybdenum carbide nanowire as an electrocatalyst for hydrogen evolution reaction, Energy Environ. Sci. 7 (2014) 387–392.